Title: Rapid genomic evolution in *Brassica rapa* with bumblebee selection in experimental evolution

Authors: Léa Frachon[1, *], Florian P. Schiestl[1]

[1]Department of Systematic and Evolutionary Botany, University of Zürich, Switzerland.

[*]***Corresponding author***:

Léa Frachon

lea.frachon@systbot.uzh.ch

Key words: fast cycling *Brassica rapa*, experimental evolution, genomic variance, rapid genomic evolution, bumblebees' selection

Abstract

Insect pollinators shape rapid phenotypic evolution of traits related to floral attractiveness and plant reproductive success. However, the underlying genomic changes remain largely unknown despite their importance in predicting adaptive responses to natural or to artificial selection. Here, based on a previous nine-generation experimental evolution study with fast cycling *Brassica rapa* plants adapting to bumblebees, we documented genomic evolution associated with the adaptive process. We performed a genomic scan of the allele frequency changes along the genome and estimated the genomic variance changes. We detected signature of selection associated with rapid changes in allelic frequencies on multiple loci, and an increase of overall genomic variance. The genomic evolution observed in nine generations was different between replicates, suggesting non-parallel evolution. Our study highlights the involvement of multiple loci in short-term pollinator adaptation, and the maintenance of genomic variance during strong natural selection by biotic factors.

Introduction

Pollinator insects are important selective agents for wild- and crop plant species due to their essential role in the reproduction of most flowering plants (Van der Niet et al. 2014). While a decline of insect pollinators has been detected in different geographical regions and insect families (Biesmeijer et al. 2006, Hallmann et al. 2017, Wagner et al. 2020), the understanding of the adaptive potential of plants to such changes remains in its infancy. Plant adaptation to pollinators typically involves traits associated with flower attractiveness such as (1) flower morphology (Anderson et al. 2016, Wessinger et al. 2016, Minaar et al. 2019), flower colour (Bradshaw et al. 2003, Sobral et al. 2015), flower scent (Schiestl 2005, Xu et al. 2012, Gervasi and Schiestl 2017), and (2) traits associated with mating system like herkogamy (Moeller and Geber 2005, Luo and Widmer 2013) or selfing (Bodbyl Roles and Kelly 2011, Ramos and Schiestl 2019). While most studies assessed the result of long-term evolutionary adaptation to pollinators, tracking the adaptive processes across generations remains rarely done. Both the resurrection approach in natural populations, growing seeds from different generations together, or experimental evolution studies, applying the same selective pressure for multiple generations, can bridge this gap. For instance, using a resurrection approach, Thomann et al. (2015) observed phenological and reproductive trait changes over 18 years in *Adonis annua* plants in response to the loss of wild bees. While this approach benefits from ecological realism in natural populations, it makes it difficult to differentiate the effect of the factor of interest from other factors such as climate, also shaping plant evolution. Gervasi and Schiestl (2017) performed experimental evolution with fast-cycling *Brassica rapa* plants evolving with different pollinators and under controlled conditions, to identify the evolutionary response to pollinator-mediated selection. They showed, within nine generations of experimental evolution, rapid plant adaptation to bumblebee pollination in phenotypic traits, such as floral volatiles, UV reflection and plant height. However, while the evolved traits have also been shown to carry substantial heritability (Zu et al. 2016, Zu and Schiestl 2017), the genomic changes underlying these rapid plant phenotypic changes are still unknown.

58 In the current context of pollinator decline and the associated changes in pollinator
59 communities, analyzing the genetic architecture of adaptation to pollinators and its association to
60 standing genetic variation is essential to understand the adaptative potential of plants in changing
61 environments (Hansen et al. 2006, Bergelson et al. 2010, Bay et al. 2017). Molecular genetic studies
62 have uncovered the molecular and genetic bases of several traits involved in pollination and pollinator
63 attractiveness such as selfing (Sicard and Lenhard 2011), pollination syndromes (Bradshaw et al. 1995,
64 Bradshaw and Schemske 2003, Streisfeld and Rausher 2009, Yuan et al. 2013, Yarahmadov et al. 2020),
65 nectar (Lin et al. 2015, Solhaug et al. 2019) and volatiles (Dudareva et al. 2006, Klahre et al. 2011, Cai
66 et al. 2016, Fattorini and Glover 2020, Lo et al. 2020). However, insects use a combination of signals
67 (shape, colour, scent) and rewards for identifying suitable flowers leading to plant adaptation based
68 on multiple traits (Schiestl and Johnson 2013). For instance, honest signals (signals associated with
69 reward) and pollination syndromes (convergent evolution of specific signal combinations selected by
70 pollinators) are good examples of evolution of multiple traits. In a context of rapid changes, genetic
71 correlation among traits may allow the synchronous response of different phenotypic traits to varying
72 patterns of selection (Hermann et al. 2013, Smith 2015, Zu and Schiestl 2017). However, we are still in
73 the beginning of understanding the genetic basis involved in the rapid evolutionary response of plants
74 to pollinator changes. Identification of genomic regions involved in plant adaptation to pollinators is
75 essential to predict the adaptive potential of plants to pollinator changes and enable breeding of more
76 attractive crop plants. In addition, an important aspect in conservation is to understand the
77 mechanisms maintaining genetic diversity within populations. In fact, standing genetic variation is an
78 important resource for rapid response to environmental changes (Barrett and Schluter 2008, Chevin
79 et al. 2010), and strong directional selection is considered to lead to the loss of genetic diversity
80 resulting in a loss of adaptive potential in populations (Barton and Keightley 2002).

81 Here, based on previous experimental evolution performed by Gervasi and Schiestl (2017) with
82 outcrossing fast-cycling *Brassica rapa* plants, we tracked the genomic changes involved in the

83 adaptative response of plants to bumblebee selection compared to hand pollinated control plants
84 (**Figure 1**), and documented the changes in genetic diversity observed in the context of strong selection
85 by estimating the genomic variance before and after experimental evolution.

86 **Methods**

87 **Plant material and experimental design.** *Brassica rapa* (Brassicacea) is an outcrossing plant with
88 genetic self-incompatibility, pollinated by diverse insects such as bumblebees, flies or butterflies (El-
89 Esawi 2017). Our study used rapid-cycling *Brassica rapa* plants (Wisconsin Fast Plants^{TM}, purchased
90 from Carolina Biological Supply Company, Burlington, USA), selected for its short life cycle of
91 approximately two months from seed to seed. We used seeds produced by the study of Gervasi and
92 Schiestl (2017), performing experimental evolution with bumblebees and control hand pollination.
93 Briefly, the pollination was carried out over nine generations either by bumblebees within cages or by
94 random hand cross-pollination. A subset of seeds produced by individual plants, proportional to the
95 total seed set of each individual within the replicates was used to generate each subsequent
96 generation. For this study, we used one seed per individual from 64 plants (half of replicate A, and half
97 of replicate B) of (1) the starting generation (generation 1; here called A1 and B1); (2) the ninth
98 generation selected by bumblebees (bumblebee treatment; here called B9A and B9B); (3) the ninth
99 generation of control hand pollination plants (control treatment; here called C9A and C9B; **Figure 1**).
100 Finally, we performed crossings between replicates A and B within each treatment, (generation 10)
101 yielding 32 individuals from the bumblebee treatment (inter-replicate crossing in bumblebee
102 treatment; here called B10) and 32 individuals from the control treatment (inter-replicate crossing in
103 control treatment; here called C10). These manual crossing are commonly used for reducing the effect
104 of potential inbreed depression on trait changes. Pollen donors and receivers were randomly assigned
105 in these crossing. Each combination of generation*treatment*replicate is called a population (*e.g.*
106 ninth generation, treatment bumblebees, replicate A called B9A is a population). A total of 256 seeds

107 from these 8 populations (first, ninth and tenth generation) were sown out in a phytotron (first
108 generation in 2017 and ninth generation as well as the inter-replicate crossing in 2019) and the leaf
109 tissue of each plant was collected for DNA extraction and whole genomic sequencing.

110 **DNA extraction and genomic characterization.** Because leaf tissue was collected in 2017 for the first
111 generation and 2019 for the last generations, we adapted the collection storage (drying vs freezing).
112 Leaf material from the first generation was dried in vacuum at 40 °C for 20 hours, and leaf material
113 from the ninth and tenth generation was stored in -80°C. A high molecular weight DNA extraction
114 (average DNA concentration of 48 ng/µL, LGC extraction protocol) and library preparation for
115 genotyping-by-sequencing (restriction enzyme MsII, insert size mean range ~215bp) was performed
116 by the LGC Genomics group Berlin. Samples were sequenced with Illumina NextSeq 500 V2 sequencer
117 using 150 paired-end reads; the alignment of our samples was performed with BWA version 0.7.12
118 against the reference genome sequence of *Brassica rapa* FPsc v1.3, Phytozome release 12
119 (https://phytozome.jgi.doe.gov/pz/portal.html) by the LGC Genomics group Berlin. The variant
120 discovery and the genotyping were realized using Freebayes v1.0.2-16 with the following parameters
121 by the LGC Genomic Group Berlin: --min-base-quality 10 –min-supporting-allele-qsum 10 –read-
122 mismatch-limit 3 –min-coverage 5 –no-indels –min-alternate-count 4 –exclude-unobserved-genotypes
123 –genotype-qualities –ploidy 2 or 3 –no-mnps –no-complex –mismatch-base-quality-threshold 10. We
124 then performed a quality trimming on the 10 chromosomes *i.e.* by discarded unassigned scaffolds from
125 the chromosomes using vcftools (Danecek et al. 2011), by removing SNPs with missing data in more
126 than 5% of the individuals (function –max-missing 0.95, *i.e.* genotype calls had to be present for at
127 least 243 samples out of 256 for a SNP to be included in the downstream analysis), and retaining only
128 bi-allelic SNPs with a minimum average Phred quality score of 15 (function –minGQ 15, **Figure S1de**).
129 We removed SNPs with a maximum average read depth of 100 (function –max-meanDP 100, **Figure**
130 **S1bc**), and discarded SNPs with a minor allele frequency (MAF) lower than 0.1 (function –maf 0.1,

131 **Figure S1a**). The final dataset contained 4'713 SNPs in ~ 283Mb genome size
132 (https://phytozome.jgi.doe.gov/pz/portal.html).

133 **Allele frequency changes and genetic drift simulation**. The allele frequencies of the reference allele
134 for the 4'713 SNPs were estimated within each 8 populations using vcftools (function –freq, Danecek
135 et al. 2011). To control for potential genetic drift during the nine generations of evolution, we
136 simulated random final allele frequencies 10'000-fold for different ranges of initial allele frequencies
137 (from 0 to 1 by an interval window of 0.01). The simulations were performed using the R environment
138 package "learnPopGen" (function "drift.selection", Revell 2019) over eight transitions between
139 generations (*i.e.* from the first generation to the ninth generation) considering 32 individuals within
140 each population for an effective size (N_e) of 16 (*i.e.* individuals contributing to the next generation, see
141 details of experimental evolution in Gervasi and Schiestl 2017), and considering an equal fitness for
142 each individual. For each SNP along the genome, we assigned their initial allele frequency value ($AF_{initial}$)
143 to the range estimated by the final allele frequency simulations (10'000 values). Finally, the observed
144 final allele frequency (AF_{final}) was compared to 10'000 simulated allele frequency values ($AF_{simulated}$) to
145 estimate a p-value for each SNP using the following equations:

146 (1) For a decrease of reference allelic frequency *i.e.* ($AF_{initial} – AF_{final}$) > 0, *pvalue* = (number of
147 simulations with $AF_{simulated} \geq AF_{final}$)/10'000
148 (2) For an increase of reference allelic frequency *i.e.* ($AF_{initial} – AF_{final}$) < 0, *pvalue* = (number of
149 simulations with $AF_{simulated} \leq AF_{final}$)/10'000
150 (3) For ($AF_{initial} – AF_{final}$) = 0, *pvalue* = 1

151 With $AF_{simulated}$ = simulated final allele frequency, $AF_{initial}$ = initial allele frequency from the
152 reference allele (first generation), and AF_{final} = observed final allele frequency for the reference allele
153 (ninth generation). The pvalues were controlled for the False Discovery Rate (fdr) of 5% using
154 Benjamini-Hochberg method implemented in R environment (Benjamini and Hochberg 1995).

155 Finally, we estimated the allele frequency changes (Δh) from the reference allele according to
156 the equation (1) for both bumblebee and control treatments:

157 $$\Delta h = \mathrm{AF}_{\mathrm{final}} - \mathrm{AF}_{\mathrm{initial}} \quad (1)$$

158 Where Δh is the allelic frequency change between the first and the ninth generation, $AF_{initial}$ is the initial
159 observed allele frequency, and AF_{final} is the observed final allele frequency at the ninth generation.

160 **Linkage disequilibrium (LD) and haplotype block structure evolution.** During selective process, an
161 increase of the linkage disequilibrium *i.e.* the non-random association of alleles between loci, is
162 expected in genomic regions strongly under selection. First, we calculated pairwise linkage
163 disequilibrium (LD) among all set of SNPs measured by the correlation coefficient between SNP pair r^2
164 within each chromosomes using VCFtools (function –geno-r2) for 256 samples within each population.
165 The associated median LD was then estimated and plotted. Finally, to understand whether changes in
166 median LD are due to random allelic associations along the genome, or aggregated in genomic regions
167 under selection, we calculated the haplotype blocks in each population using plink1.9 with the
168 following parameters: --blocks no-pheno-req –maf 0.07 –blocks-max-kb 200. This method estimates
169 the length of theses blocks with "strong LD" considering the allelic association D' metrics between 0.7
170 and 0.98 according to (Gabriel et al. 2002).

171 **Candidate genes.** We identified 171 candidate genes associated with 187 SNPs with significant allele
172 frequency changes (fdr < 0.05) during bumblebee selection. Because the median linkage disequilibrium
173 in bumblebee treatment is ~4kb, we retrieved the annotated genes around 4kb (2 kb upstream and 2
174 kb downstream) for 187 SNPs and extracted the gene description using phytozome.jgi.doe.gov.

175 **Genome-wide variance changes.** The genomic variance among individuals within each population was
176 estimated using principal component analysis (PCA) on scaled and centered genotype data (pcadapt
177 package in R environment, function pcadapt, Privé et al. 2020). In order to unravel the changes in

178 genomic variance over nine generations, we performed the PCA (1) on the total number of SNPs (4713
179 SNPs), and (2) on 187 SNPs showing significant allele frequency changes under bumblebee selection in
180 on or another replicate (fdr < 0.05). To compare genomic variance among populations, we estimated
181 the area of the polygon formed by scatter plots of axis 1 and 2 of each population for the full dataset
182 (4713 SNPs) and the subset of 187 SNPs using R package tidyverse and splancs (Wickhman et al. 2019,
183 Rowlingson and Diggle 2022). The relative area is the ratio between the polygon area within each
184 population and the polygon area circumventing all the points of the PCA.

185

186 **Results**

187 **Genomic changes during experimental evolution.** In our study, we observed allele frequency changes
188 (Δh) over nine generations in both bumblebee and control treatments (**Figure 2**). However, the
189 strongest (Δh > 0.5) and most significant (frd < 0.05) changes were observed in the bumblebee
190 treatment for the replicate A on 32 SNPs (4 SNPs for the replicate B in the bumblebee treatment, 0
191 SNP and 3 SNPs for replicate A and B respectively in the control treatment). Overall, the significant
192 changes observed in replicate A for the bumblebee treatment (fdr < 0.05), regardless of its strength,
193 involved 42-fold more SNPS than in the control treatment (4 SNPs with significant changes in the
194 control treatment, and 171 SNPs in the bumblebee treatment, **Figure 2**). In replicate B, we did not
195 observe difference in allelic frequency changes between the two treatments (21 SNPs with significant
196 changes in the control, and 19 in the bumblebee treatment considering fdr < 0.05, **Figure 2**).

197 As expected, the evolutionary process is associated with an increase of linkage disequilibrium
198 in the bumblebee treatment, but also in the control treatment. The decay of the median linkage
199 disequilibrium was slower in both treatments in the ninth generation than in the first one (**Figure S2A**).
200 Within the bumblebee treatment, we observed a slower decay of LD in replicate A than in B as
201 expected with the observed stronger allele frequency changes (**Figure S2A**). The decays of LD in inter-

202 replicate crossing were slower in both treatments compared to the ninth generation (**Figure S2A**).
203 Moreover, we observed a decrease of the number of haplotype blocks, *i.e.*, genomic regions with
204 strongly linked alleles, over nine generations (from 786 and 780 haplotype blocks for replicate A and B
205 respectively in the first generation, to 563 and 648 haplotype blocks for replicate A and B respectively
206 in the ninth generation of the control treatment, and 478 and 600 for replicate A and B respectively in
207 the ninth generation of the bumblebee treatment) associated with an increase of their length (**Figure**
208 **S2BC**, **Table S1**). We observed 743 and 696 haplotype blocks in control and bumblebee treatments
209 respectively in the inter-replicate crossing (**Figure S2BC, Table S1**).

210 Overall, the SNPs involved in the evolutive responses are independent between replicates, and
211 between treatments (**Figure 3**). For instance, among the 171 SNPs with significant allele frequency
212 changes in replicate A in bumblebee treatment, 164 SNPs are unique of this population, whereas 5
213 SNPs are shared with the control treatment in replicate B, and 3 SNPs are shared with the bumblebee
214 treatment in replicate B (**Figure 3**).

215 **Identity of candidate genes underlying genomic evolution to bumblebees.** After retrieving the
216 annotated genes around 4kb (2kb upstream, 2kb downstream) for 187 SNPs with significant allele
217 frequency changes in the bumblebee treatment (fdr < 0.05), we obtained a list of 171 candidate genes
218 (**Dataset1**). Briefly, we found genes with biological functions that may be involved in the emission of
219 volatiles (ABC transporter G), in the regulation of flowering time (B3), or in shoot architecture (UCH).
220 In addition, some genes are involved in the response to different biotic and abiotic stresses
221 (METACASPASE-2, PUB, Pum, PAT8, BON). Finally, some candidate genes do not have a known
222 biological function.

223 **Genomic variance changes.** To assess the variation of genomic variance across generation, we
224 performed a genomic principal component analysis (PCA) on the full set of SNPs (4'713 SNPs). We
225 observed a structuration of our samples determined by populations *i.e*. generations, treatments, and

226 replicates (**Figure 4A**). Along the two first principal components (PCs) axis, explaining 24.5% of the total
227 genomic variance, all individuals from the two replicates of generation one were grouped together,
228 and individuals from the ninth generations were clearly separated from the first generation, but they
229 were also separated between both treatments and replicates (**Figure 4A**). In genomic space, individuals
230 from the inter-replicate crossing fell between those from the scatterplot formed by replicates A and B
231 of generation nine for both treatments (**Figure 4A**). We estimated the genomic variance of our
232 populations by calculating the area of polygons in the genomic space formed by the first two PCs. We
233 observed a 2-fold and 4-fold increase in genomic variance (polygon area) between the first and the
234 ninth generation in replicates A and B respectively in bumblebee treatment, and a 0.5-fold and 2-fold
235 increase in replicates A and B respectively in control treatment (**Figure 4C**). In the inter-replicate
236 crossing for both treatments, we observed a 0.8-fold and 7.7-fold (3.9-fold considering only samples
237 without outliers) increase of the polygon area compared to replicate A in first generation, in control
238 and bumblebee treatments respectively (**Figure 4C**).

239 In the reduced dataset including significant allele frequency changes in bumblebee treatment
240 (both replicate A and B, *i.e.* 187 SNPs), we observed a clear distinction between individuals from the
241 bumblebee treatment and other populations (**Figure 4B**). Indeed, individuals from the first generation
242 and the control treatment are clustered closely together, and the individuals from bumblebee
243 treatment were clearly separated in the genomic space (**Figure 4B**). For the first generation and control
244 treatment, we observed a higher genomic variance (polygon relative area) for PCA performed on the
245 sub-dataset than the one performed with the full dataset (**Figure 4C**). In the bumblebee treatment, we
246 observed different pattern regarding the replicate; a small increase of the genomic variance (polygon
247 relative area) in replicate A, and a decrease in replicate B and inter-crossing (**Figure 3C**). These genomic
248 regions drove the evolutionary process observed in bumblebee selection, while maintaining genetic
249 diversity in the treatment under selection.

250 **Discussion**

251 Understanding pollinator-mediated evolutionary genomics of flowering plants and its impact
252 on standing genetic variation within the genome remains an important challenge in conservation.
253 Here, we screened for the genomic consequences of biotic selection in an experimental evolution
254 experiment by sequencing genome-wide SNP markers in *Brassica rapa* plant individuals before and
255 after nine generations of selection by bumblebees, and under random hand-pollination. As shown
256 previously at the level of the phenotype, this primarily outcrossing plant rapidly adapt to specific
257 pollinators (Gervasi and Schiestl 2017). We documented the signature of directional selection driven
258 by bumblebee pollinators with significant allele frequency changes at several loci. Interestingly, we
259 documented a maintenance of standing genetic variation across the genome, a finding challenging the
260 classical selective sweep model.

261 In agreement with the previously demonstrated phenotypic evolution in the fast-cycling *Brassica*
262 *rapa* experimental system (Gervasi and Schiestl 2017), we have shown genomic evolution across nine
263 generations. The here documented changes in allele frequencies, the increase of linkage disequilibrium
264 and the number of haplotype blocks, underlined the importance of pollinators in shaping plant rapid
265 genomic evolution. Some significant candidate genes identified in our study have biological functions
266 in line with the phenotypic evolution of traits observed by Gervasi and Schiestl (2017). For instance,
267 while this previous study highlighted increase in scent emission and plant height driven by bumblebee
268 pollination, we identified candidate genes who, or at least their family, are known to be involved in
269 emission of volatile organic compounds, like ABC transporter G family (ABCG35, ABCG38, ABCG1,
270 ABCB19, Adebesin et al. 2017, Hao et al. 2021), in shoot architecture like Ubiquitin C-terminal
271 hydrolase (UCH, Yang et al. 2007), or in growth and development like AUXIN-RESPONSIVE PROTEIN-
272 RELATED, or TREHALOSE-PHOSPHATE PHOSPHATASE E-RELATED (Figueroa and Lunn 2016). The U-box
273 protein is also an interesting candidate gene due to its involvement in different developmental and

274 physiological processes such as self-incompatibility, defence, or abiotic stress response (Wang et al.
275 2015). Moreover, we found significant allele frequency changes associated with flowering time like a
276 B3 transcription regulator (Swaminathan et al. 2008) or UCH (Hayama et al 2021). While Gervasi &
277 Schiestl (2017) did not observe any difference in flowering time between bumblebee and control
278 treatment in the last generation, flowering time is an important phenological trait involved in plant-
279 pollinator matching (Forrest 2005, Hegland et al. 2009). It is therefore likely that pollinators induce
280 flower phenological shift. Overall, our study highlighted the potential involvement of multiple loci in
281 rapid adaption to bumblebees, which agrees with studies highlighting such a genetic architecture
282 underlying floral evolution (Fishman et al. 2002, Yuan et al. 2013, Fishman et al. 2015, Smith 2015,
283 Campitelli et al. 2017). However, further analysis using higher quality of sequencing and the full
284 characterization of associated phenotypic and phenological traits (allowing a genome-wide association
285 approach) and functional validation of the genes are required to draw more solid conclusions about
286 the genetic basis of evolutionary changes induced by bumblebee selection. Moreover, among loci
287 under-selection, the lack of annotation and the unknown functions of some genes highlighted the need
288 to deepen our knowledge on genes involved in plant-pollinator interactions.

289 We found that the extent of genomic changes observed during evolutionary processes was
290 different between replicates suggesting non-parallel evolution (Bolnick et al. 2018). This result is in line
291 with the observed phenotypic evolution in Gervasi and Schiestl (2017) with significant differences
292 among replicates in the bumblebee treatment for different phenotypic traits. Such evolution was
293 observed in natural population of *Senecio lautus* with similar phenotypic variation regulated by
294 variation in genomic space (James et al. 2021). However, we observed significant changes in allele
295 frequencies only in one replicate, indicating that it is difficult to clearly distinguish potential non-
296 parallel evolution from a “two-speed” parallel evolution (*i.e.* the second replicate will follow the same
297 evolutionary path in the upcoming generations). Longer experimental evolution, with more replicates

298 and individuals are needed to understand the evolutionary pattern mediated by biotic factors such as
299 bumblebees.

300 Finally, we observed an increase of the overall genomic variance despite the selection imposed by
301 bumblebees during experimental evolution (2017), and the small effective size of populations. This
302 increase in overall genomic variance was observed among individuals in both bumblebee-pollinated
303 replicates (B9A and B9B), as well as in the inter-replicate crossing (B10). This pattern might be
304 explained by the polygenic model with a weaker selection acting on multiple standing variants (soft
305 sweep) and by multiple loci underlying individual phenotypic trait evolutionary changes. An increased
306 number of studies demonstrate the importance of polygenic adaptation (Pritchard and di Rienzo 2010,
307 Csilléry et al. 2018, Barghi et al. 2020) related to the infinitesimal model (reviewed in Barton et al.
308 2017), where local adaptation is driven by small allele frequency changes in multiple loci. This outcome
309 is supported by recent work observing the maintenance of standing genetic variation during long-term
310 artificial selection on chicken weight, mainly explained by selection acting on highly polygenic
311 architecture (Sheng et al. 2015). However, deepened analyses are needed using newly developed
312 models to validate such hypothesis (Berg et al. 2014, Boyle et al. 2017, Wieters et al. 2021). Multiple
313 genes underlying phenotypic variation are widely emphasized in plants with the advances of GWAs
314 (Barghi et al. 2020), however the interplay of evolutionary forces on these genes and their involvement
315 in the potential maintenance of standing genetic variation is still poorly understood and deserve
316 further studies.

317 **Conclusion**

318 We revealed important genomic changes on multiple loci during bumblebee selection during only
319 nine generations. Our study is a first step into the understanding of the complex genomic mechanisms
320 involved in rapid evolutionary adaptation to biotic factors, and we advocate further analyses to
321 understand (1) the genetic architecture underlying phenotypic and phenological variation, (2)

322 pleiotropic effects of quantitative-trait locus in rapid adaptation and (3) the mechanisms behind a
323 maintenance of genetic variance. We also underline the importance of better characterizing the gene
324 functions involved in plant-pollinator interactions. Overall, pollinators constitute complex patterns of
325 selection which deserve more attention for predicting the adaptive responses of wild and crop plant
326 species to their decline.

327

328 **Acknowledgements**

329 We thank Jörg Vogt for the first-generation DNA extraction, and the LGC Genomic group Berlin for the
330 DNA extraction of other samples, the sequencing and bioinformatic treatment. We thank Cyril Zipfel
331 for discussion regarding candidate genes. We thank Loren Rieseberg and Marius Rösti for their useful
332 comments on a previous version of the draft. Finally, we thank the University of Zürich for their
333 financial support.

334

335 **Author Contributions**

336 L.F. and F.S. designed the research. L.F. performed the DNA extraction, statistical analyses and wrote
337 the manuscript. L.F. and F.S. reviewed and edit the manuscript.

338

339 **References**

340 Adebesin, F. *et al.* Emission of volatile organic compounds from petunia flowers is facilitated by an ABC
341 transporter. *Science*. **356**, 1386-1388 (2017).
342 Anderson, B., Pauw, A., Cole, W. W. & Barrett S. C. H. Pollination, mating and reproductive fitness in a
343 plant population. *Journal of Evolutionary Biology*. **29**, 1631–1642 (2016).
344 Barghi, N., Hermisson, J. & Schlötterer, C. Polygenic adaptation: a unifying. *Nature Reviews Genetics*.
345 21, 769-781 (2020).
346 Barrett, R. D. H. & Schluter, D. Adaptation from standing genetic. *TRENDS in Ecology and Evolution*.
347 23(1), 38-44 (2008).
348 Barton, N. H. & Keightley, P.D. Understanding quantitative genetic variation. *Nature Reviews Genetics*.
349 3, 11-21 (2002).
350 Barton, N. H., Etheridge, A.M. & Véber, A. The infinitesimal model: Definition, derivation, and
351 implications. *Theoretical Population Biology*. 118, 50-73 (2017).
352 Bay, R. A. *et al*. Predicting responses to contemporary environmental change using evolutionary
353 response architectures. *The American naturalist*. **189**(5), 463-473 (2017).
354 Benjamini, Y. & Hochberg Y. Controlling the false discovery rate: a practical and powerful approach to
355 multiple testing. *Journal of Royal Statistical Society: Series B*. **57**(1), 289-300 (1995).

356 Berg, J. J & Coop, G. A population genetic signal of polygenic adaptation. *PloS Genet.* **10**(8), e1004412
357 (2014).
358 Bergelson, J. & Roux, F. Towards identifying genes underlying ecologically relevant traits in Arabidopsis
359 thaliana. *Nature Reviews Genetics.* **11**, 867-879 (2010).
360 Biesmeijer, J. C. *et al*. Parallel declines in pollinators and insect-pollinated plants in Britain and the
361 Netherlands. *Science*. **313**, 351-354 (2006).
362 Bodbyl Roles, S. A. & Kelly, J. K. Rapid evolution caused by pollinator loss in *Mimulus guttatus.*
363 *Evolution*. **65**(9), 2541–2552 (2011).
364 Bolnick D. I., Barrett R. D. H., Oke K. B., Rennison D. J., Stuart Y. E. (Non)Parallel Evolution. *Annual*
365 *Review of Ecology, Evolution, and Systematics*. 19, 303-330 (2018).
366 Boyle, E. A., Li, Y. I. & Pritchard J. K. An expanded view of complex traits: from polygenic to
367 omnigenic. *Cell*. 169, 1177-1186 (2017).
368 Bradshaw, H. D. & Schemske, D. W. Allele substitution at a flower colour locus produces a pollinator
369 shift in monkeyflowers. *Nature*. **426**, 176-178 (2003).
370 Bradshaw, H. D., Wilbert, S. M., Otto, K. G. & Schemsket, D. W. Genetic mapping of floral traits
371 associated with reproductive isolation in monkeyflowers (*Mimulus*). *Nature*. **376**, 762-765
372 (1995).
373 Cai, J., Zu, P. & Schiestl F. P. The molecular bases of floral scent evolution under artificial selection:
374 insights from a transcriptome analysis in Brassica rapa. *Scientific Reports*. **6**, 36966 (2016).
375 Campitelli, B. E., Kenney, A. M., Hopkins, R., Soule, J., Lovell, J. T. & Juenger, T.E. Genetic mapping
376 reveals an anthocyanin biosynthesis pathway gene potentially influencing evolutionary
377 divergence between two subspecies of scarlet gilia (*Ipomopsis aggregata*). *Molecular Biology*
378 *and Evolution*. **35**(4), 807–822 (2017).
379 Chevin, L. M., Lande, R. & Mace, G. M. Adaptation, plasticity, and extinction in a changing environment:
380 towards a predictive theory. *PLOS biology*. **8**, e1000357 (2010).
381 Csilléry, K., Rodriguez-Verdugo, K., Rellstab, C. & Guillaume, F. Detecting the genomic signal of
382 polygenic adaptation and the role of epistasis in evolution. *Molecular Ecology*. **27**, 606-612
383 (2018).
384 Danecek, P., Auton A., Abecasis, G., Albers C., A., Banks, E., DePristo, M. A., Handsaker, R., Lunter, G.,
385 Marth, G., Sherry, S. T., McVean, G., Durbin, R. and 1000 Genomes Project Analysis Group. The
386 variant call format and VCFtools. *Bioinformatics* **27**, 2156–2158 (2011).
387 Dudareva, N., Negre, F., Nagegowda, D. A. & Orlova, I. Plant Volatiles: Recent Advances and Future
388 Perspectives. *Critical Reviews in Plant Sciences*. **25**, 417–440 (2006).
389 El-Esawi, M. A. Genetic diversity and evolution of Brassica genetic resources: from morphology to novel
390 genomic technologies – a review. *Plant Genetic Resources: Characterization and Utilization*.
391 **15**(5), 388–399 (2017).
392 Fattorini, R. & Glover, B. J. Molecular Mechanisms of Pollination Biology. *Annual Review of Plant*
393 *Biology*. **71**, 487-515 (2020).
394 Figueroa C. M., Lunn J. E. A Tale of Two Sugars: Trehalose 6-Phosphate and Sucrose. *Plant Physiology*.
395 **172**, 7-27 (2016).
396 Fishman, L., Beardsley, P. M., Stathos, A., Williams, C. F. & Hill, J. P. The genetic architecture of traits
397 associated with the evolution of self-pollination in Mimulus. *New Phytologist*. **205**, 907–917
398 (2015).
399 Fishman, L., Kelly, A. J. & Willis, J. H. Minor quantitative trait loci underlie floral traits associated with
400 mating system divergence in mimulus. *Evolution*. **56**(11), 2138–2155 (2002).
401 Forrest, J. R. K. Plant – pollinator interactions and phenological change: what can we learn about
402 climate impacts from experiments and observations? *Oikos*. **124**, 4-13 (2005).
403 Gabriel, S. B. et al. The structure of haplotype blocks in the Human genome. *Science*. **296**, 2225-2229
404 (2002).

405 Gervasi, D. D. L. & Schiestl, F. P. Real-time divergent evolution in plants driven by pollinators. *Nature*
406 *communications*. **8**, 14691 (2017).
407 Hallmann, C. *et al*. More than 75 percent decline over 27 years in total flying insect biomass in
408 protected areas. *PloS ONE*. **12**(10), e0185809 (2017).
409 Hansen, T. F. The evolution of genetic architecture. *Annual Review of Ecology, Evolution, and*
410 *Systematics*. **37**, 123–57 (2006).
411 Hao, R., Yang, R., Zhang, Z., Zhang, Y., Chang, J. & Qiu, C. Identification and specific expression patterns
412 in flower organs of ABCG genes related to floral scent from *Prunus mume*. *Scientia Horticulturae*.
413 **288**, 110218 (2021).
414 Hayama R., Yang P., Valverde F., Mizoguchi T., Furutani-Hayama I., Vierstra R. D., Coupland G.
415 Ubiquitin carboxyl-terminal hydrolases are required for period maintenance of the circadian
416 clock at high temperature in Arabidopsis. *Scientific Reports*. **9**, 17030 (2021).
417 Hegland, S. J., Nielsen, A., Lázaro, A., Bjerknes, A.-L. & Totland, Ø. How does climate warming affect
418 plant-pollinator interactions? *Ecology Letters*. **12**, 184-195 (2009).
419 Hermann, K., Klahre, U., Moser, M., Sheehan, H., Mandel, T. & Kuhlemeier, C. Tight genetic linkage of
420 prezygotic barrier loci creates a multifunctional speciation island in *Petunia*. *Current Biology*. **23**,
421 873–877 (2013).
422 James, M. E., Wilkinson, M. J., Bernal, D. M., Liu, H., North, H. L., Engelstädter, J., Ortiz-Barrientos, D.
423 Phenotypic and genotypic parallel evolution in parapatric ecotypes of *Senecio*. *Evolution*.
424 10.1111/evo.14387 (2021).
425 Klahre, U. *et al*. Pollinator choice in Petunia depends on two major genetic loci for floral scent
426 production. *Current Biology*. **21**, 730-739 (2011).
427 Lin, W. *et al*. Nectar secretion requires sucrose phosphate synthases and the sugar transporter
428 SWEET9. *Nature*. **508**, 546-549 (2015).
429 Lo, S., Fatokun, C., Boukar, O., Gepts, P., Close, T. J., & Muñoz-Amatriain, M. Identification of QTL for
430 perenniality and floral scent in cowpea (*Vigna unguiculata* [L.] Walp.). *PloS ONE*. **15**(4),
431 e0229167 (2020).
432 Luo, Y. & Widmer, A. Herkogamy and its effects on mating patterns in *Arabidopsis thaliana. PloS ONE*.
433 **8**(2), e57902 (2013).
434 Minnaar, C., Anderson, V., de Jager, M. L., & Karron, J. D. Plant–pollinator interactions along the
435 pathway to paternity. *Annals of Botany*. **123**, 225–245 (2019).
436 Moeller, D. A. & Geber, M. A. Ecological context of the evolution of self-pollination in *Clarkia xantiana*:
437 population size, plant communities, and reproductive assurance. *Evolution*. **59**(4), 786–799
438 (2005).
439 Pritchard, J. K. & Di Rienzo, A. Adaptation – not by sweeps alone. *Nature Reviews Genetics*. **11**(10),
440 665–667 (2010).
441 Privé, F., Luu, K., Vilhjálmsson, B. J. & Blum, M. G. B. Performing highly efficient genome scans for local
442 adaptation with R package pcadapt version 4. *Molecular Biology and Evolution*. **37**(7), 2153–
443 2154 (2020).
444 Ramos, S. E. & Schiestl, F. P. Rapid plant evolution driven by the interaction of pollination and
445 herbivory. *Science*. **364**, 193–196 (2019).
446 Revell, L. J. learnPopGen: An R package for population genetic simulation and numerical analysis.
447 *Ecology and Evolution*. **9**, 7896–7902 (2019).
448 Rowlingson, B., Diggle, P. splancs: Spatial and Space-Time Point Pattern Analysis. *R package version*
449 *2.01-43*. https://CRAN.R-project.org/package=splancs (2022).
450 Schiestl, F. P. On the success of a swindle: pollination by deception in orchids. *Naturwissenschaften*.
451 **92**, 255–264 (2005).
452 Schiestl, F.P. & Johnson, S. D. Pollinator-mediated evolution of floral signals. *Trends in Ecology &*
453 *Evolution*. **28**, 307-315 (2013).

Sheng, Z., Pettersson, M. E., Honaker, C. F., Siegel, P. B. & Carlborg, O. Standing genetic variation as a major contributor to adaptation in the Virginia chicken lines selection experiment. *Genome Biology*. **16**, 219 (2015).

Sicard, A. & Lenhard, M. The selfing syndrome: a model for studying the genetic and evolutionary basis of morphological adaptation in plants. *Annals of Botany*. **107**, 433–1443 (2011).

Smith, S. D. Pleiotropy and the evolution of floral integration. *New Phytologist*. **209**, 80–85 (2015).

Sobral, M., Veiga, T., Domínguez, P., Guitián, J.A., Guitián, P., & Guitián, J. M. Selective pressures explain differences in flower color among Gentiana lutea populations. *PloS ONE*. **10**(7), e0132522 (2015).

Solhaug, E. M. *et al*. An integrated transcriptomics and metabolomics analysis of the Cucurbita pepo nectary implicates key modules of primary metabolism involved in nectar synthesis and secretion. *Plant Direct*. **3**, e00120 (2019).

Streisfeld, M. A. & Rausher, M. D. Genetic changes contributing to the parallel evolution of red floral pigmentation among Ipomoea species. *New Phytologist*. **183**, 751–763 (2009).

Swaminathan, K., Peterson, K. & Jack, T. The plant B3 superfamily. *Trends in Plant Science*. **13**, 647-655 (2008).

Thomann, M., Imbert, E. & Cheptou, P.O. Is rapid evolution of reproductive traits in Adonis annua consistent with pollinator decline? *Acta Oecologica*. **69**, 161-166 (2015).

Van der Niet, T., Peakall, R. & Johnson, S.D. Pollinator-driven ecological speciation in plants: new evidence and future perspectives. *Annals of Botany*. **113**, 199–211 (2014).

Wagner, D. L., Grames, E. M., Forister, M. L., Berenbaum, M. R. & Stopak, D. Insect decline in the Anthropocene: Death by a thousand cuts. *PNAS*. **118**(2), e2023989118 (2020).

Wang C., Duan W., RamuliMaquina Riquicho A., Jing Z., Liu T., Hou X., Li Y. Genome-wide survey and expression analysis of the *PUB* family in Chinese cabbage (*Brassica rapa* ssp*. pekinesis*). *Molecular genetics and genomics*. **290**, 2241-2260 (2015).

Wessinger, C. A. & Hileman, L. C. Accessibility, constraint, and repetition in adaptive floral evolution. *Developmental Biology*. **419**, 175–183 (2016).

Wickham, H. *et al*. Welcome to the tidyverse. Journal of Open. *Source Software*. **4**(43), 1686 (2019).

Wieters, B., Steige, K. A., He, F., Koch, E. M., Ramos-Onsins, S. E., Gu, H., Guo, Y. L., Sunyaev, S. & de Meaux, J. Polygenic adaptation of rosette growth in *Arabidopsis thaliana. PloS Genet*. **17**(1), e1008748 (2021).

Xu, S., Schlüter, P. M., Grossniklaus, U. & Schiestl, F. P. The genetic basis of pollinator adaptation in a sexually deceptive Orchid. *PloS Genet*. **8**(8), e1002889 (2012).

Yang P., Smalle J., Lee S., Yan N., Emborg T. J., Vierstra R. D. Ubiquitin C-terminal hydrolases 1 and 2 affect shoot architecture in Arabidopsis. *The Plant Journal*. **51**, 441-457 (2007).

Yarahmadov, T., Robinson, S., Hanemian, M., Pulver, V. & Kuhlemeier, C. Identification of transcription factors controlling floral morphology in wild Petunia species with contrasting pollination syndromes. *The Plant Journal*. **104**(2), 289–301 (2020).

Yuan, Y. W., Byers, K. J. R. P. & Bradshaw, H. D. J. The genetic control of flower–pollinator specificity. *Current Opinion in Plant Biology*. **16**, 422–428 (2013).

Zu, P. & Schiestl, F. P. The effects of becoming taller: direct and pleiotropic effects of artificial selection on plant height in Brassica rapa. *The Plant Journal*. **89**, 1009–1019 (2017).

Zu, P., Blanckenhorn, W. U. & Schiestl, F. P. Heritability of floral volatiles and pleiotropic responses to artificial selection in *Brassica rapa*. *New Phytologist*. **209**, 1208–1219 (2016).

503 **Legends**

504

505 **Figure 1. Experimental evolution design.** Partial experimental evolution design from Gervasi and
506 Schiestl (2017) from the first generation (G1) to the ninth generation in control (C9) and bumblebee
507 treatment (B9). The tenth generation was obtained by inter-replicate crossing (C10 and B10).
508 Population of *Brassica rapa* fast cycling used for seedling sequencing are coloured. The abbreviation
509 and the colours assigned to the populations are unchanged along the manuscript. The number of
510 seedlings (n) sequenced per population is indicated.

511

512 **Figure 2. Allele frequency changes during experimental evolution.** (**A**) Comparison of the allele
513 frequency changes (Δh) between the bumblebee treatment (*x-axis*) and the control treatment (*y-axis*).
514 The grey dots represent the 4'713 SNPs. Replicate A is in light grey, replicate B in darker grey. The
515 significant changes are highlighted in blue and green (see the legend in the figure for details).
516 Comparison of initial (first generation) and final (ninth generation) allele frequencies in the control
517 treatment for both replicate A **(B)** and replicate B **(D)**, and in the bumblebee treatment for both
518 replicate A **(C)** and replicate B **(E)**. The grey dots represent the non-significant changes in allele
519 frequencies between generations. The grey solid lines indicate the maximum (upper line) or minimum
520 (lower line) of final simulated allele frequencies obtained by 10'000 simulations of random genetic
521 drift (over nine generations, N_e=16). The color dots represent important changes with *fdr* < 0.05.

522

523 **Figure 3. Intersection of genomic variants under selection between treatment and replication.** The
524 UpSet plot illustrates the genomic variants involved in the evolution of *Brassica rapa* in control and
525 bumblebee treatment for both replicates A and B. On the left (Set Size), the number of significant
526 genomic variants involved in evolutionary response of *B. rapa* in different populations is indicated. The
527 dots indicate that the genomic variants are involved in the evolutionary response only in a particular
528 population, while the vertical lines indicate that the genomic variants are involved in the evolutionary
529 processes in several populations. The number of genomic variants involved in unique population or in
530 different populations is indicated in the upper part of the figure.

531

532 **Figure 4. Genomic variance within populations. (A-B)** Position of the 256 individuals in the genomic
533 space from the principal component analysis (PCA) performed on their genotypes (GT). The PCAs were
534 performed **(A)** on the total set of SNPs (4'713 SNPs), and **(B)** on the 187 SNPs with significant changes
535 in allele frequency during bumblebee selection (fdr < 0.05). The label of the population is shown on

their centroid. Polygons linking outer points of the scatter plot are displayed for all populations. For the generation 10 in bumblebee treatment, the polygon linking points without outlier is represented in grey (**C**) Bar plots presenting area values of polygons for the different populations. The filled bars are the values from PCA performed on the full dataset (4’713 SNPs), and the dashed ones on the reduced dataset (187 SNPs). The legend colours are indicated in the bottom right of the figure. For the generation 10 in bumblebee treatment, the polygon areas based on all samples are represented in blue, and the one based on samples without outliers are in grey.

562 **Figure 1**

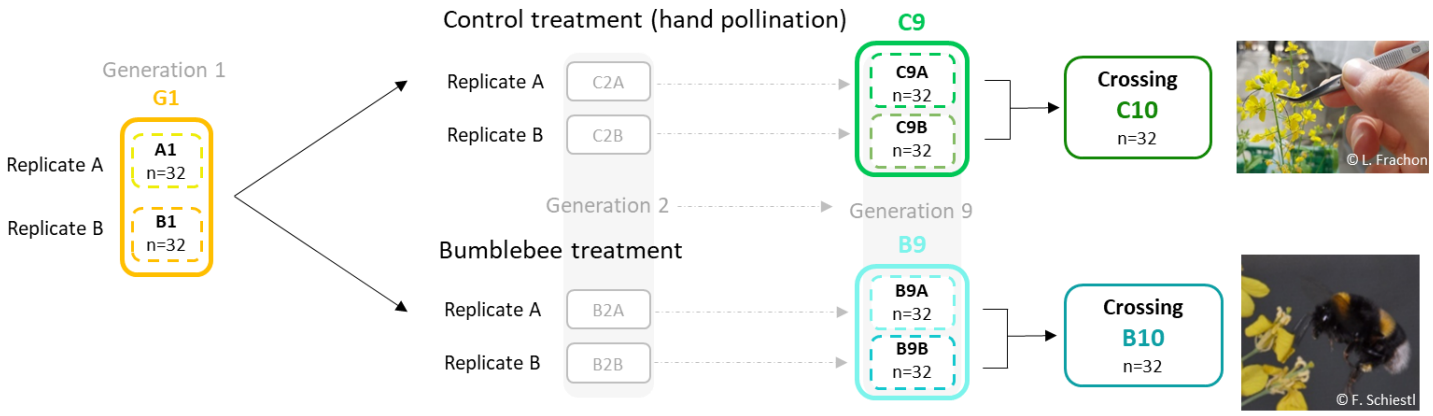

563

564 **Figure 2**

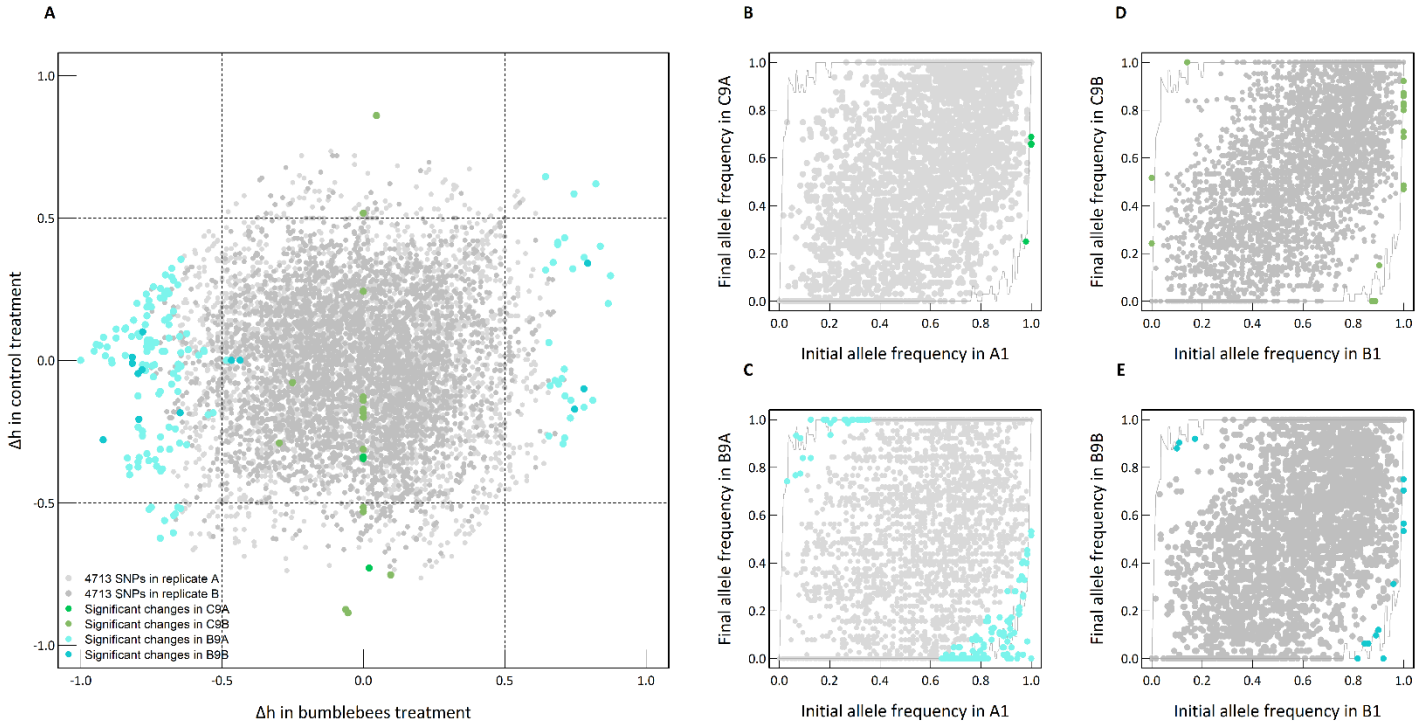

565

566

567

568

569

570

571 **Figure 3**

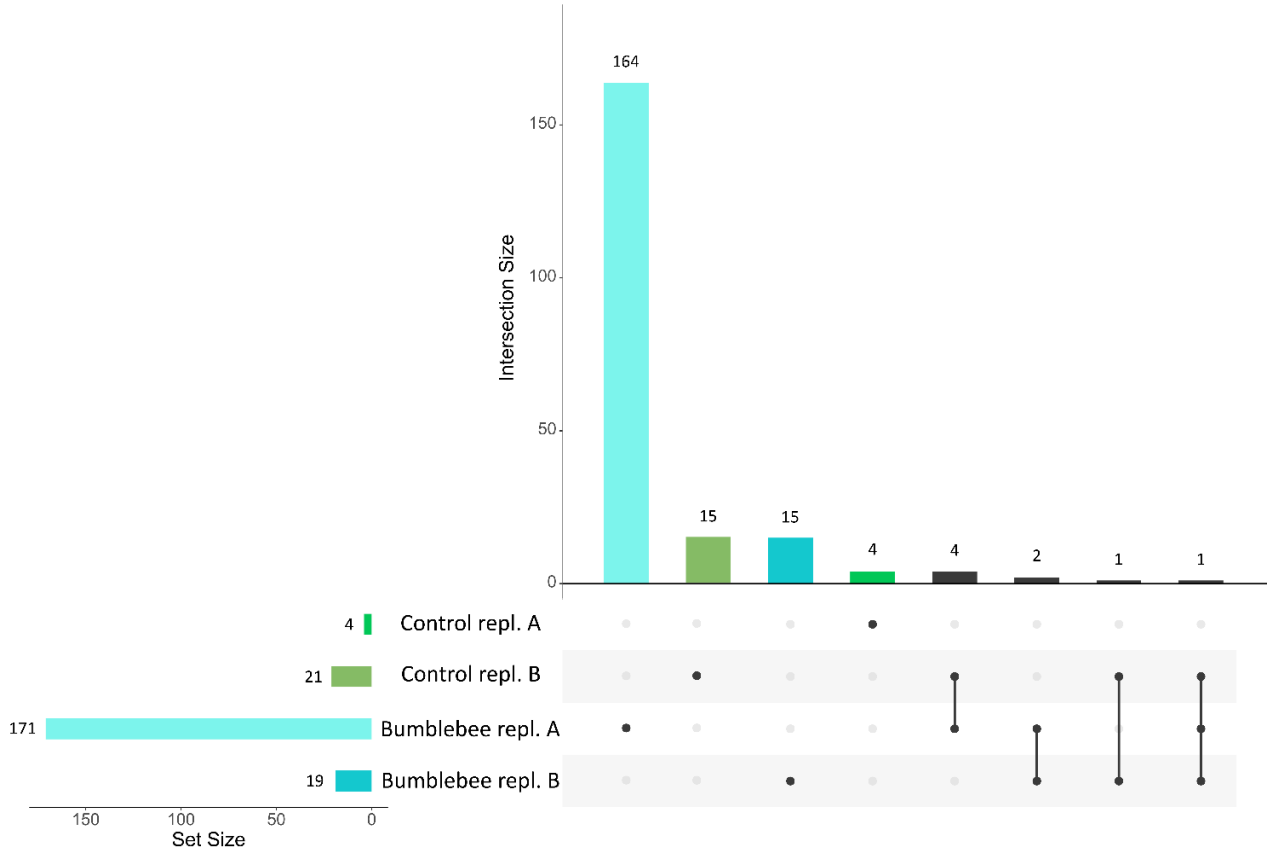

572

573 **Figure 4**

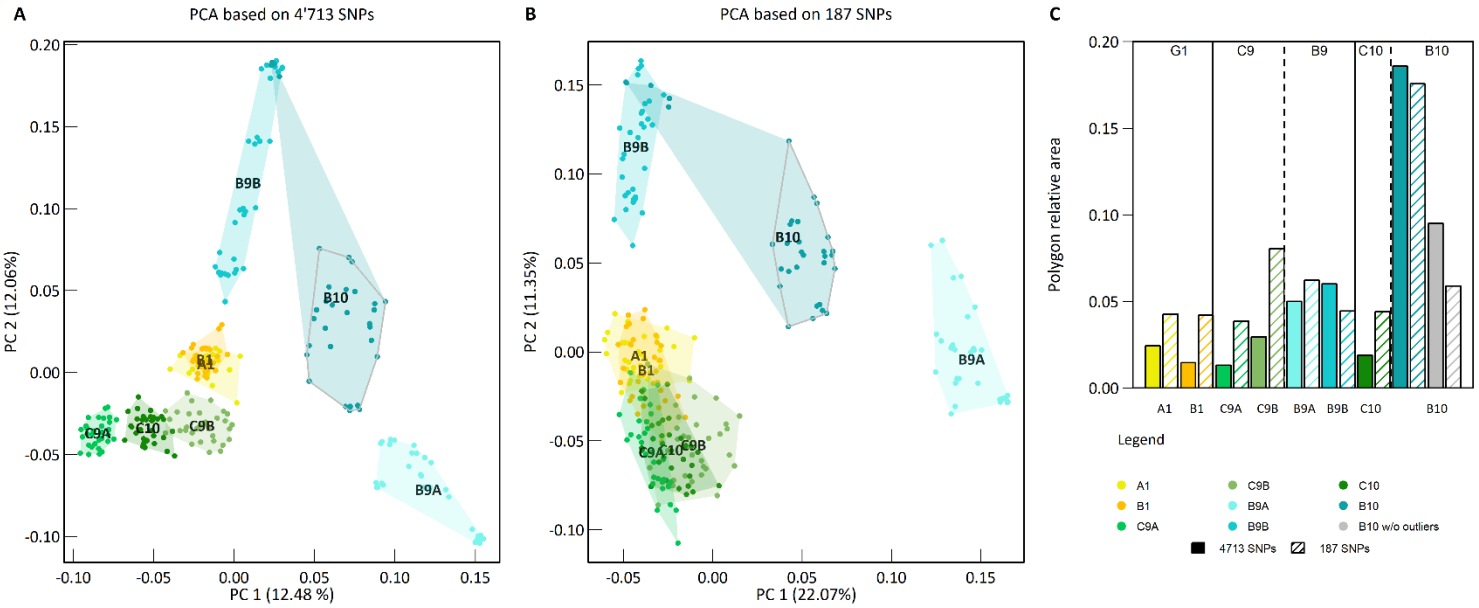

Supplementary information

Figure S1. Distribution of filtered genomic data for our final dataset of 4'713 SNPs. (a) Distribution of the minor allele frequency, (b) distribution of average read depth (DP) per SNPs, (c) distribution of the average read depth (DP) per individual, (d) distribution of the average genotype quality (GQ), (e) different thresholds of the minimum average GQ as a function of the number of SNPs in the final dataset. The red line indicates the chosen value in our study (--minGQ = 15).

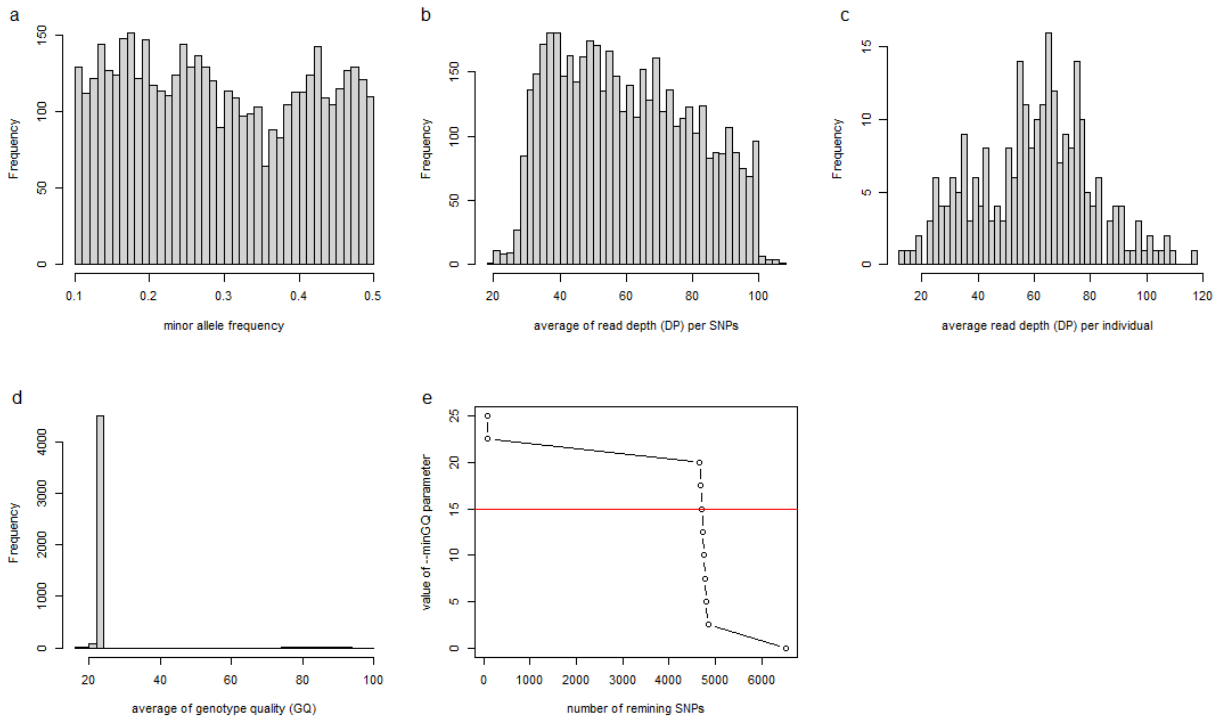

Figure S2. Linkage disequilibrium and haplotype block structure. (A) Distribution of the median pairwise linkage disequilibrium (r^2) for each population by distance between two SNPs (kb). **(B)** Number of haplotype block calculated within each population **(C)** Average length (kb) of haplotype blocks per population (more details Table S1).

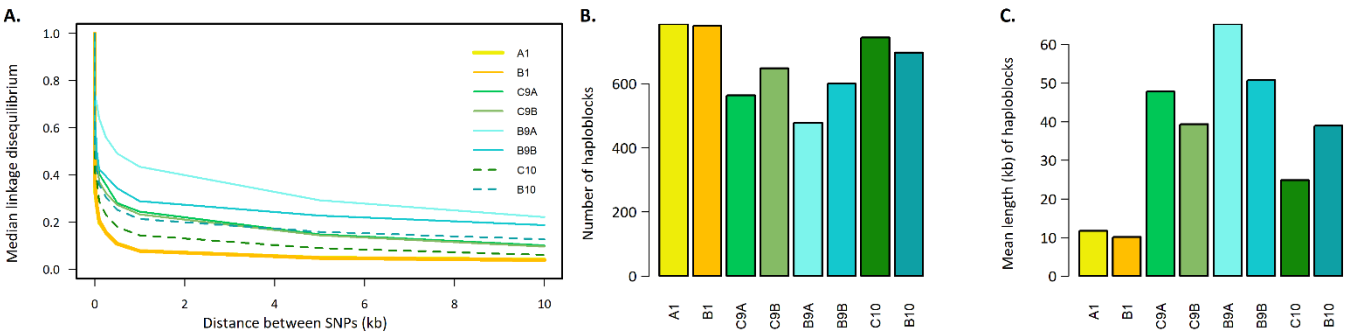

588 **Table S1. Haplotype blocks.** For each population, the number of haplotype blocks, the mean (+- sd)
589 of the number of SNPs per haplotype block, and the length (in kb) of haplotype blocks.

590

	Nber blocks	mean length/block	median length/block	mean nber of SNP/block	median nber of SNP/block
A1	786	11.75	0.11	3.13	3
B1	780	10.14	0.1	3.06	3
C9A	563	47.81	0.69	4.07	3
C9B	648	39.37	0.2	3.91	3
B9A	478	65.33	20	4.33	4
B9B	600	50.71	1.13	4.12	3
C10	743	24.87	0.15	3.53	3
B10	696	38.94	0.17	3.87	3